Current Biology, Volume *28*

Supplemental Information

SMC1α Substitutes for Many Meiotic Functions of SMC1β but Cannot Protect Telomeres from Damage

Uddipta Biswas, Michelle Stevense, and Rolf Jessberger

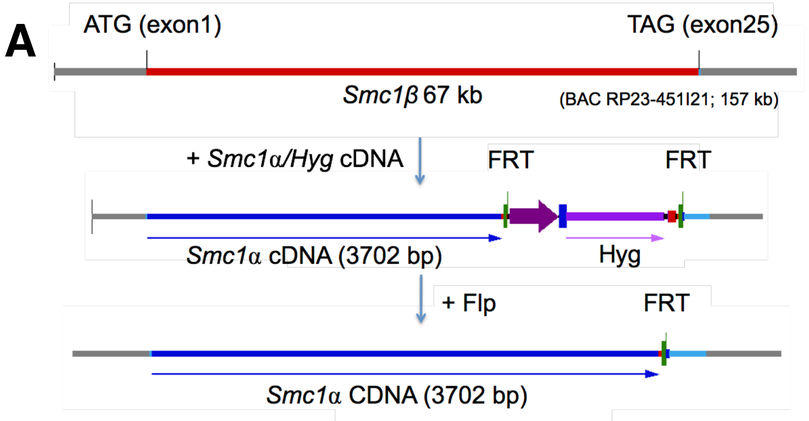
A
ATG (exon1)
TAG (exon25)
Smc1β 67 kb
(BAC RP23-451I21; 157 kb)
+ Smc1α/Hyg cDNA
FRT
FRT
Smc1α cDNA (3702 bp)
Hyg
+ Flp
FRT
Smc1α CDNA (3702 bp)

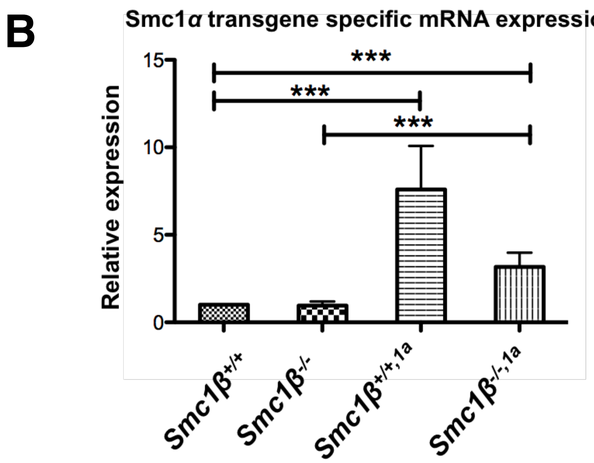
B
Smc1α transgene specific mRNA expression
Relative expression
***
***
***
Smc1β+/+
Smc1β-/-
Smc1β+/+,1a
Smc1β-/-,1a

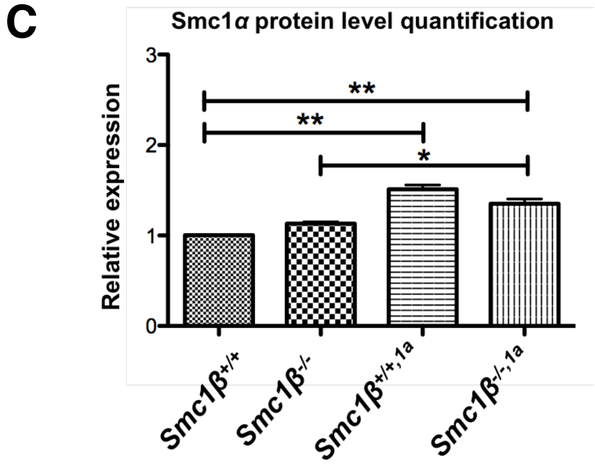
C
Smc1α protein level quantification
Relative expression
**
**
*
Smc1β+/+
Smc1β-/-
Smc1β+/+,1a
Smc1β-/-,1a

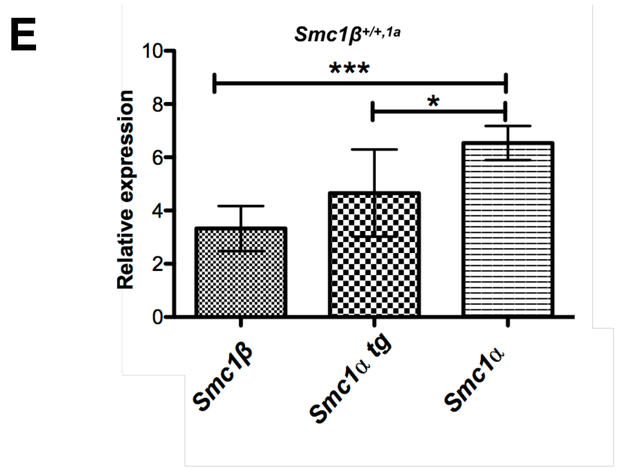
E
Smc1β+/+,1a
Relative expression
***
*
Smc1β
Smc1α tg
Smc1α

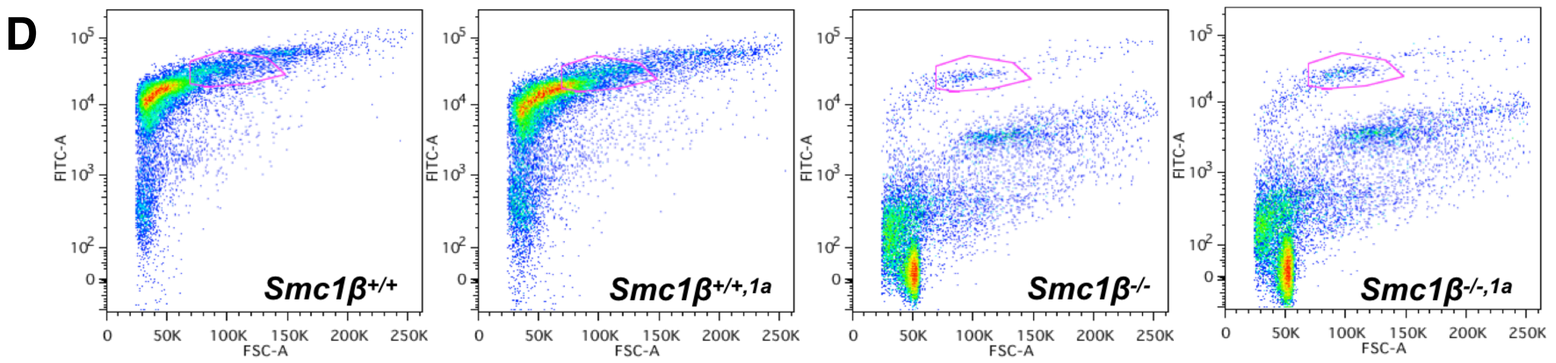
D
FITC-A
FSC-A
Smc1β+/+
Smc1β+/+,1a
Smc1β-/-
Smc1β-/-,1a

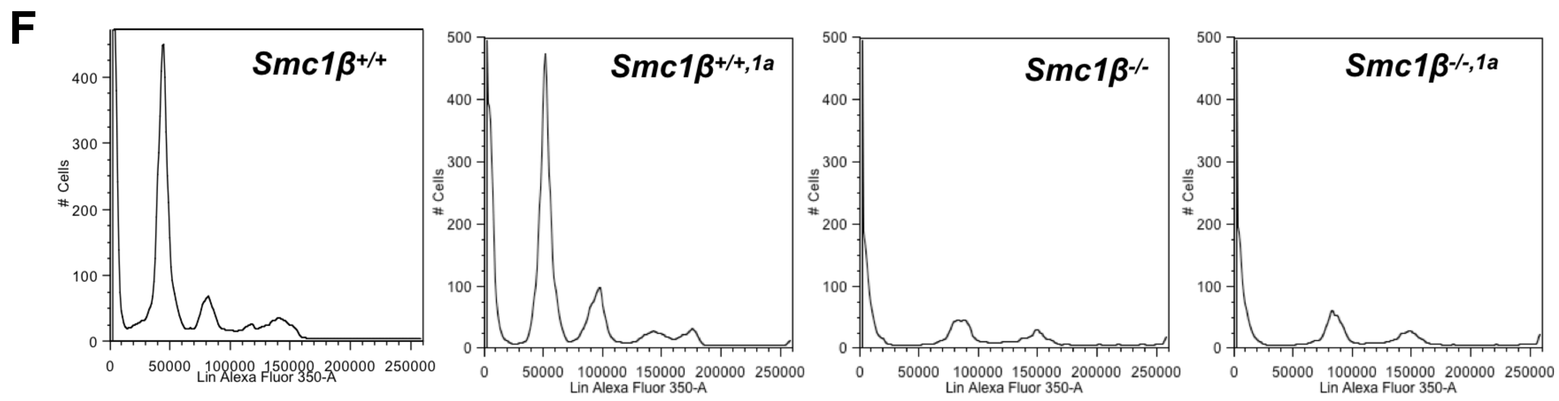
F
Cells
Lin Alexa Fluor 350-A
Smc1β+/+
Smc1β+/+,1a
Smc1β-/-
Smc1β-/-,1a

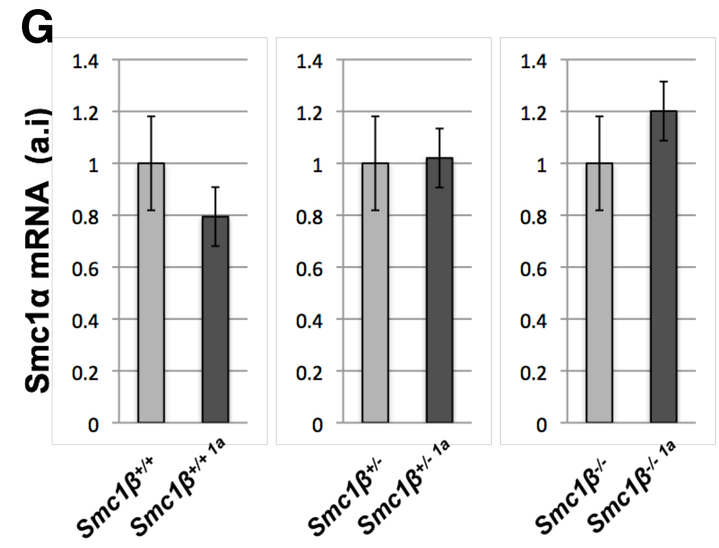
G
Smc1α mRNA (a.i)
Smc1β+/+
Smc1β+/+ 1a
Smc1β+/-
Smc1β+/- 1a
Smc1β-/-
Smc1β-/- 1a

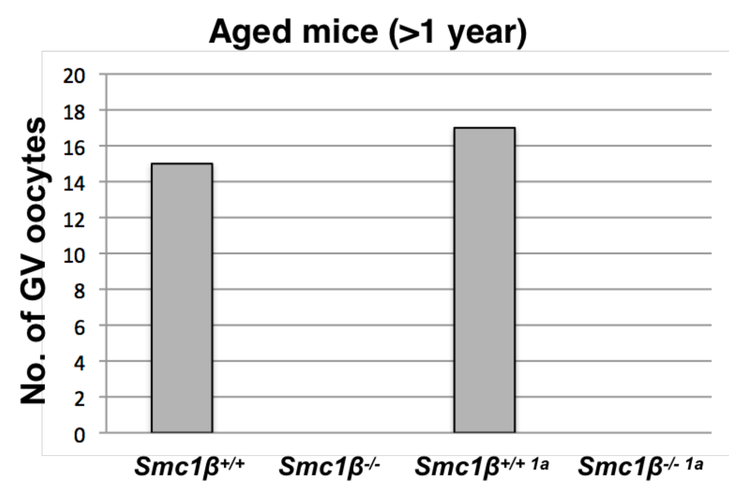
H
Aged mice (>1 year)
No. of GV oocytes
Smc1β+/+
Smc1β-/-
Smc1β+/+ 1a
Smc1β-/- 1a

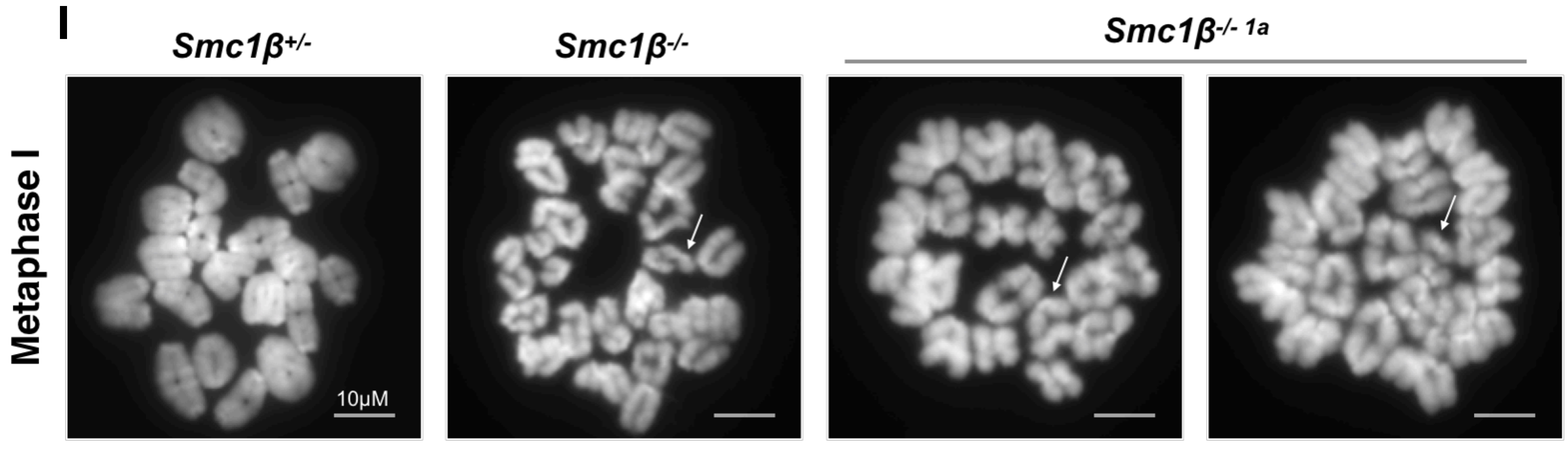
I
Smc1β+/-
Smc1β-/-
Smc1β-/- 1a
Metaphase I
10μM

Figure S1. Experimental approach. Related to Figure 1: (A) Schematic diagram for SMC1α BAC generation. The *Smc1α* cDNA-FRT-hyg-FRT template was cloned into the R6k plasmid. Next the cDNA-FRT-hyg-FRT fragment was released from R6k and integrated into the BAC RP23-451I21. For the integration into the BAC, homology arms of each 40 bp upstream of the *Smc1β* ATG and 40 bp downstream of the *Smc1β* TAG were used. Before the pronuclear microinjection, the selection marker (hyg) was removed using Flp recombinase. (B) Sorting strategy for the protein and RNA isolation. GFP positive spermatocytes are sorted from all the genotypes (C) Cell cycle analysis of the spermatocytes of all genotypes. (D to F) Transgene mRNA and protein quantification: (D) Quantification of transgene specific *Smc1α* expression. *Smc1α* expression levels were normalised to *Smc1α* levels in $Smc1\beta^{+/+}$ spermatocytes. According to Bonferroni's multiple comparison test the mean values for *Smc1α* expression of all genotypes ($Smc1\beta^{+/+,1a}$: 7.5881 +/- 2.49 ; $Smc1\beta^{-/-}$: 0.9558 +/- 0.3378 and $Smc1\beta^{-/-,1a}$: 3.174 +/- 0.8114) are significantly different ($p<0.05$). (E) Quantification of SMC1α protein levels (N=2). The ratio was calculated by normalizing SMC1α with tubulin levels within the same genotypes and for comparison the relative levels were normalized to $Smc1\beta^{+/+}$ levels. $Smc1\beta^{+/+,1a}$: 1.5 (mean) +/- 0.006 (SD) ; $Smc1\beta^{-/-}$: 1.132 +/- 0.0018 and $Smc1\beta^{-/-,1a}$: 1.351 +/- 0.053) ($p<0.05$). (F) Expression levels in FACS-sorted 4N $Smc1\beta^{+/+1\alpha}$ spermatocytes of *Smc1α* (endogenous and transgene), *Smc1α* transgene only, and *Smc1β was* measured by real-time PCR. Turkey's multiple comparison test showed no statistically significant difference between *Smc1α* transgene (tg) and *Smc1β* expression ($p > 0.05$), while the total *Smc1α* expression was higher as expected ($p < 0.05$). (G to H) Smc1βprom-Smc1α transgenic oocytes: (G) mRNA levels of Smc1βprom-Smc1α transgene in adult oocytes. qPCR data for adult female $Smc1\beta^{+/+}$, $Smc1\beta^{+/-}$ *or* $Smc1\beta^{-/-}$ mice strains, which were genotyped as either negative (light grey) or positive (dark grey) for the Smc1βprom-Smc1α transgene. Each bar represents the level of the Smc1βprom-Smc1α transgene mRNA in 50 GV oocytes (a.i.). The data was normalised to the house-keeping gene Rsp16 and the data was set to 1 for each Smc1βprom-Smc1α transgene negative mouse. (H) Number of GV oocytes in aged mice. Graph shows number of GV oocytes recovered from both ovaries of aged mice between 61 to 67 weeks old. One representative data set is presented. The same was observed in multiple independent experiments. (I) Chromosome spreads of adult oocytes**.** Images show representative examples of chromosome spreads at metaphase I (MI). Mice were between 6 to 8 weeks old. $Smc1\beta^{+/-}$ and $Smc1\beta^{-/-}$ cells were used as controls, to illustrate loss of cohesion in the $Smc1\beta^{-/-}$ strain. Two examples of $Smc1\beta^{-/-,1a}$ cells are presented. Cells were stained with DAPI (scale bar 10 μM).

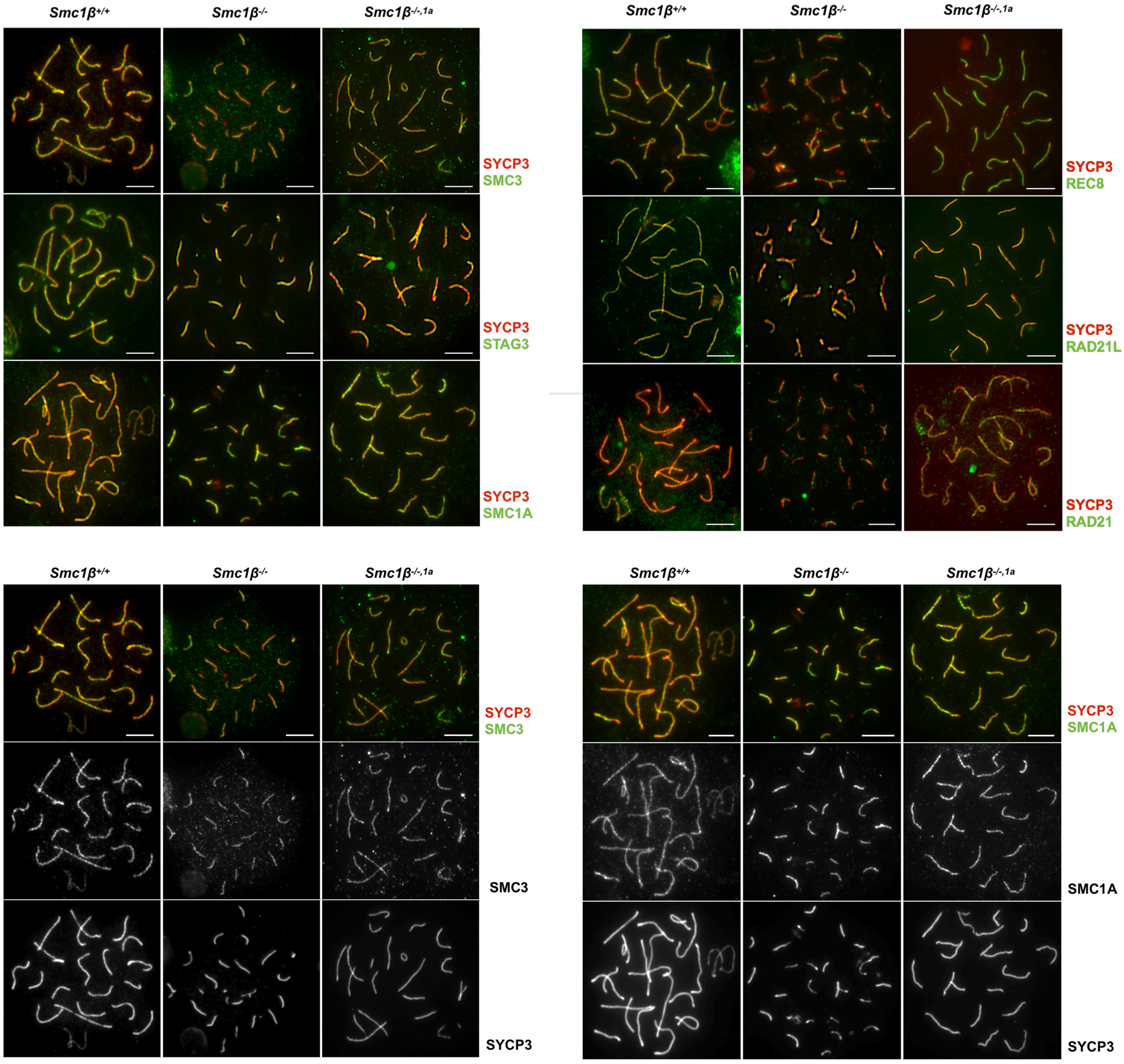
Smc1β+/+
Smc1β-/-
Smc1β-/-,1a
SYCP3
SMC3
SYCP3
STAG3
SYCP3
SMC1A
Smc1β+/+
Smc1β-/-
Smc1β-/-,1a
SYCP3
REC8
SYCP3
RAD21L
SYCP3
RAD21
Smc1β+/+
Smc1β-/-
Smc1β-/-,1a
SYCP3
SMC3
SMC3
SYCP3
Smc1β+/+
Smc1β-/-
Smc1β-/-,1a
SYCP3
SMC1A
SMC1A
SYCP3

Figure S2. Presence of cohesin proteins. Related to Figure 2. Spermatocyte chromosome spreads of *Smc1β*$^{+/+}$, *Smc1β*$^{-/-}$ and *Smc1β*$^{-/-,1a}$ mice were probed with anti-SYCP3 along with anti-SMC3, anti-STAG3, anti-SMC1α, anti-REC8 anti-RAD21L or anti-RAD21 (scale bar: 5 µm). All cohesins are labeled in green. Lower panels: Single channel images of spermatocyte chromosome spreads of *Smc1β*$^{+/+}$, *Smc1β*$^{-/-}$ and *Smc1β*$^{-/-,1a}$ mice probed with anti-SYCP3 along with anti-SMC3 or anti-SMC1α; (scale bars: 5 µm).

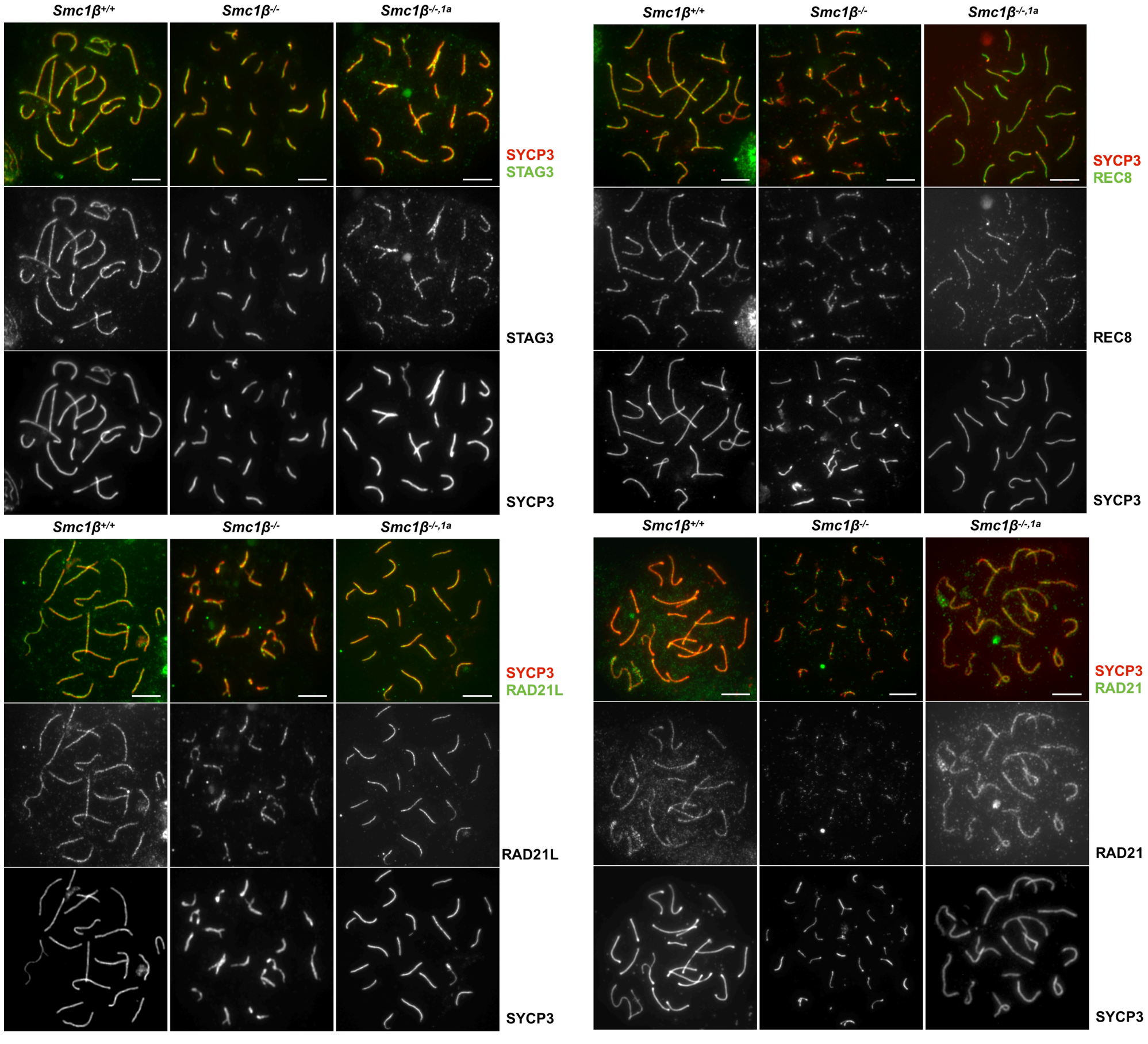
Smc1β+/+
Smc1β-/-
Smc1β-/-,1a
SYCP3
STAG3
STAG3
SYCP3
Smc1β+/+
Smc1β-/-
Smc1β-/-,1a
SYCP3
REC8
REC8
SYCP3
Smc1β+/+
Smc1β-/-
Smc1β-/-,1a
SYCP3
RAD21L
RAD21L
SYCP3
Smc1β+/+
Smc1β-/-
Smc1β-/-,1a
SYCP3
RAD21
RAD21
SYCP3

Figure S3. Presence of cohesin proteins. Related to Figure 2. Single channel images of spermatocyte chromosome spreads of *Smc1β*$^{+/+}$, *Smc1β*$^{-/-}$ and *Smc1β*$^{-/-,1a}$ mice probed with anti-SYCP3 along with anti-STAG3, anti-REC8, anti-RAD21L, or anti-RAD21; (scale bars: 5 µm).

A

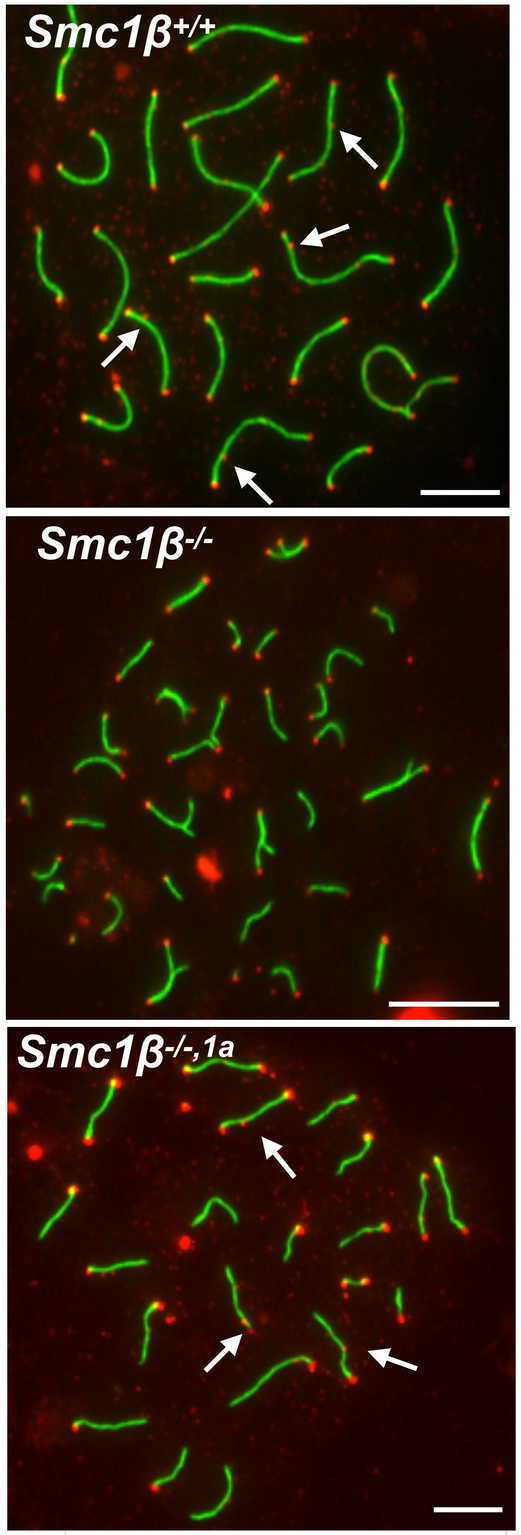
Smc1β+/+
Smc1β-/-
Smc1β-/-,1a
SYCP3
CDK2

B

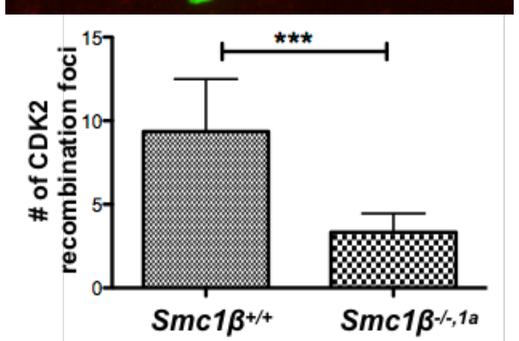
***
# of CDK2 recombination foci
15
10
5
0
Smc1β+/+
Smc1β-/-,1a

C

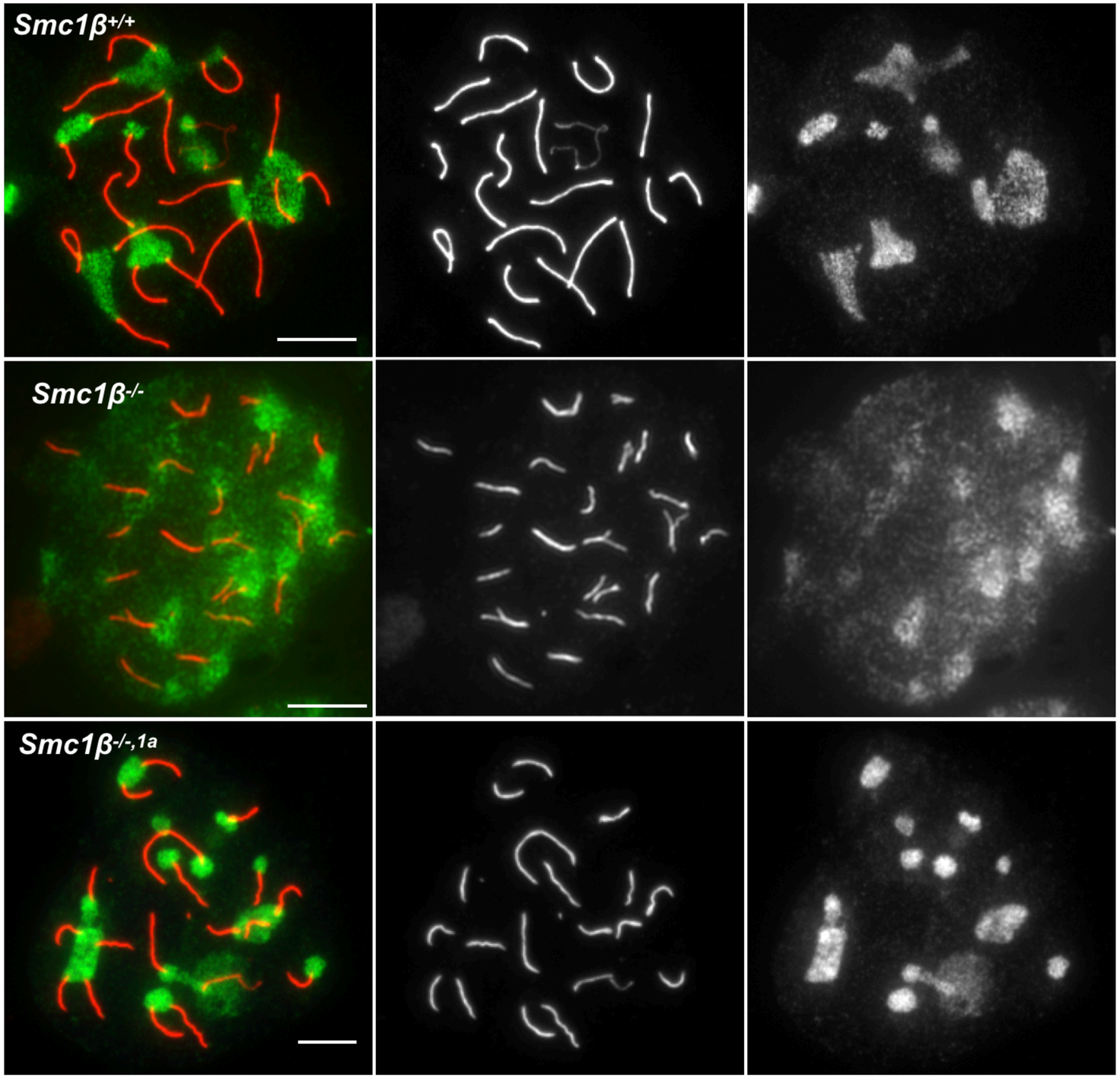
Smc1β+/+
Smc1β-/-
Smc1β-/-,1a
H3K9me3 SYCP3
SYCP3
H3K9me3

Figure S4. Analysis of CDK2 foci. Related to Figure 3. (A) Spermatocyte chromosome spreads of *Smc1β*$^{+/+}$, *Smc1β*$^{-/-}$ and *Smc1β*$^{-/-,1a}$ mice were stained with anti-CDK2 (red) and with anti-anti-SYCP3 (green) for AEs/LEs, (scale bar: 5 μm) (B) Graphical representation of CDK2 recombination foci of spermatocyte spreads as measured using the image J software; (*Smc1β*$^{+/+}$: N=50, 9.36 (average foci number, +/- 3.128 SD); *Smc1β*$^{-/-,1a}$: N=36, 3.33 *(*+/- 1.12); $p < 0.05$). (C) H3K9me3 localization. Spermatocyte chromosome spreads of *Smc1β*$^{+/+}$ and *Smc1β*$^{-/-,1a}$ mice were stained with anti-H3K9me3 (green) for heterochromatin and with anti-anti-SYCP3 (red) for AEs/LEs. (scale bar: 5 μm).

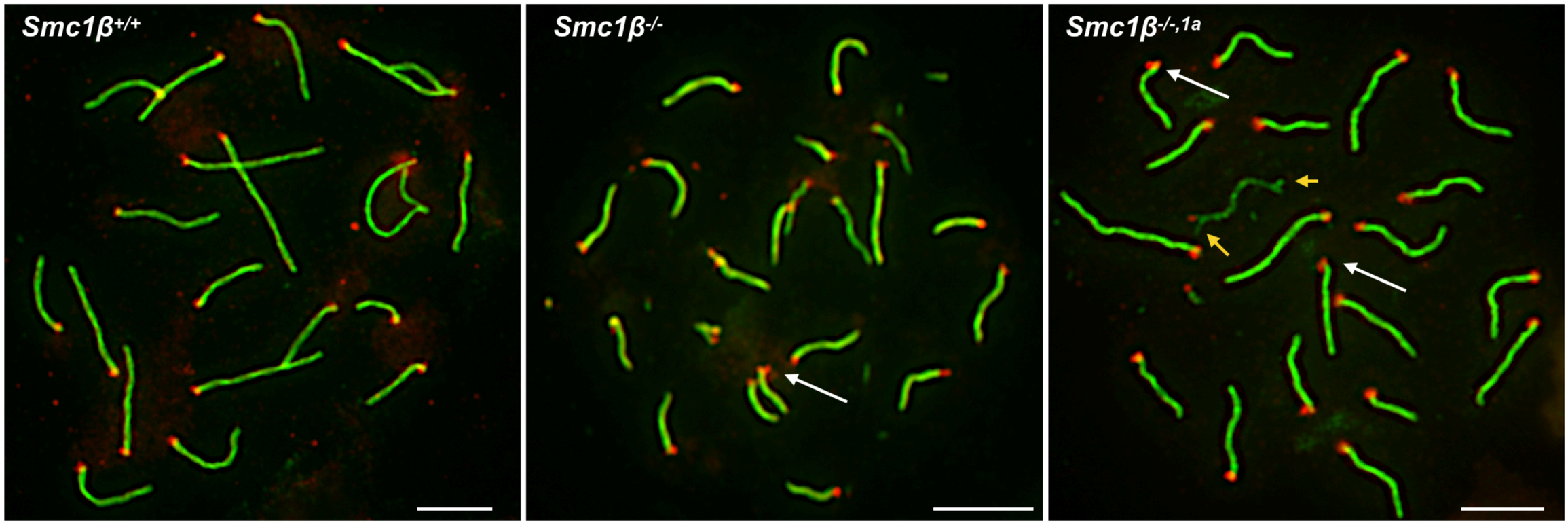

ACA SYCP3 ACA SYCP3 ACA SYCP3

Figure S5. Centromere/pericentromere staining. Related to figure 5. Spermatocyte chromosome spreads of *Smc1β*$^{+/+}$, *Smc1β*$^{-/-}$ and *Smc1β*$^{-/-,1a}$ mice, stained with anti-SYCP3 (green) for AEs/LEs and anti-ACA (red); white arrows indicate abnormal centromere structures, yellow arrows show examples of loss of centromeric or telomeric cohesion seen at the X chromosome; (scale bar: 5 μm).

A

Average Telomere Aberrations/Cell

Genotype	End-end Associations	Stret-ches	Solitary Telo Signals	Telo-less Ends	Overall	# of Telomeres Analyzed
Smc1β$^{-/-}$	0.06	1.92	5.60	5.92	13.69	533
Smc1β$^{-/-1a}$	0.50	2.33	3.91	3.83	10.58	492
p-value	0.25	0.51	0.02	0.31	0.05	

B

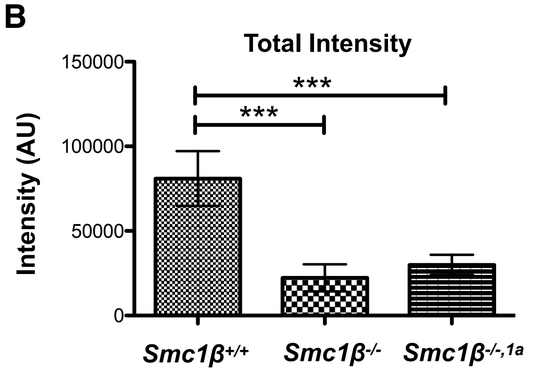

C

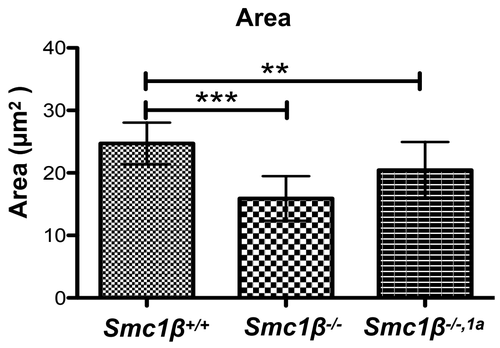

D

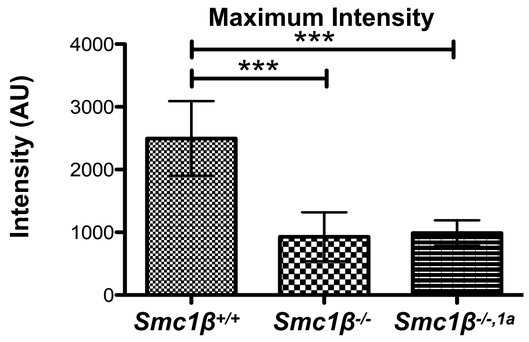

E

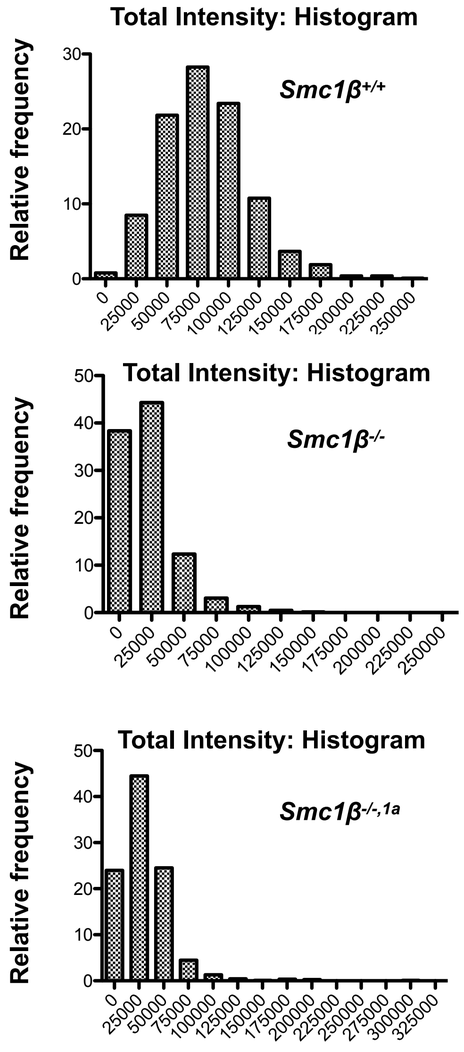

F

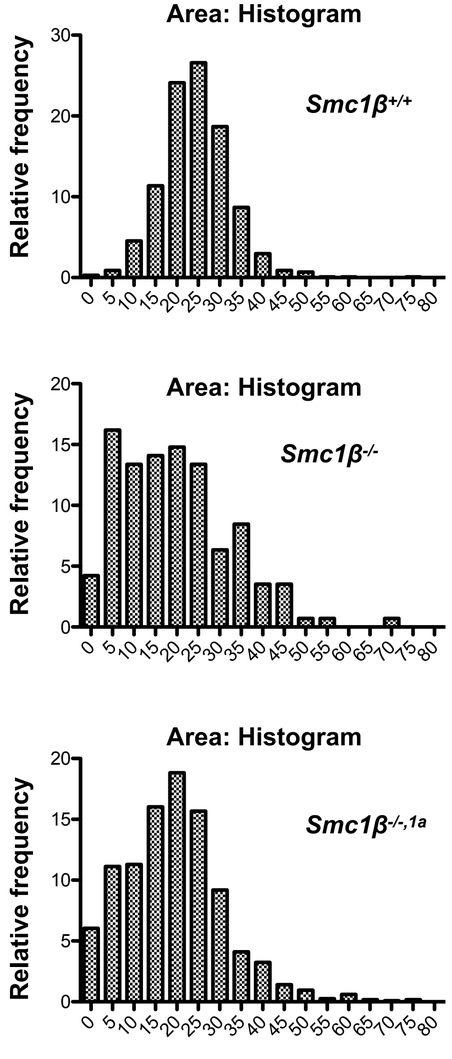

Figure S6. Telomere analysis. Related to Figure 6. (A) Average number of specific telomere aberrations and of all (overall) telomere aberrations per cell. The p-values reflect the difference between the two genotypes for each type of aberrations or overall. (B) Graphical representation of telomere length (Telo FISH signal intensity) of spermatocyte spreads as measured using the image J software; (*Smc1β*$^{+/+}$: N=1012, number of telomeres, 80971 a.u. average total intensity (+/- 16217 SD); *Smc1β*$^{-/-}$: N=623, 22279 (+/- 7974); *Smc1β*$^{-/-,1a}$: N=1142, 29969 (+/- 5967)). The pairwise differences were not statistically relevant (p >0.05). (C) Graphical representation of telomere area (Telo FISH signal) of spermatocyte spreads measured using the image J software; (*Smc1β*$^{+/+}$: N=1012, 24.72 (average area) (+/- 3.33 SD); *Smc1β*$^{-/-}$: N=623, 15.89 (+/- 3.599); *Smc1β*$^{-/-,1a}$: N=1142, 20.46 (+/- 4.483)). All pairwise differences were statistically relevant (p <0.05). (D) Graphical representation of maximum telomere intensity (Telo FISH signal) of spermatocyte spreads as measured using image J software; (*Smc1β*$^{+/+}$: N=1012 telomeres, 2540 maximum intensity (+/- 840 SD); *Smc1β*$^{-/-}$: N=623, 927 (+/- 577); *Smc1β*$^{-/-,1a}$: N=1142, 1026 (+/- 470)). The pairwise differences were not statistically relevant (p >0.05). (E) and (F) Histogram of telomere length and telomere area distribution profiles of spermatocyte spreads as measured using image J software; (*Smc1β*$^{+/+}$: N=1012, *Smc1β*$^{-/-}$: N=623, *Smc1β*$^{-/-,1a}$: N=1142). According to Chi-square analysis both telomere length and telomere area histogram profiles of *Smc1β*$^{+/+}$,*Smc1β*$^{-/-}$ and *Smc1β*$^{-/-,1a}$ spermatocytes are statistically significantly different, p<0.00001.

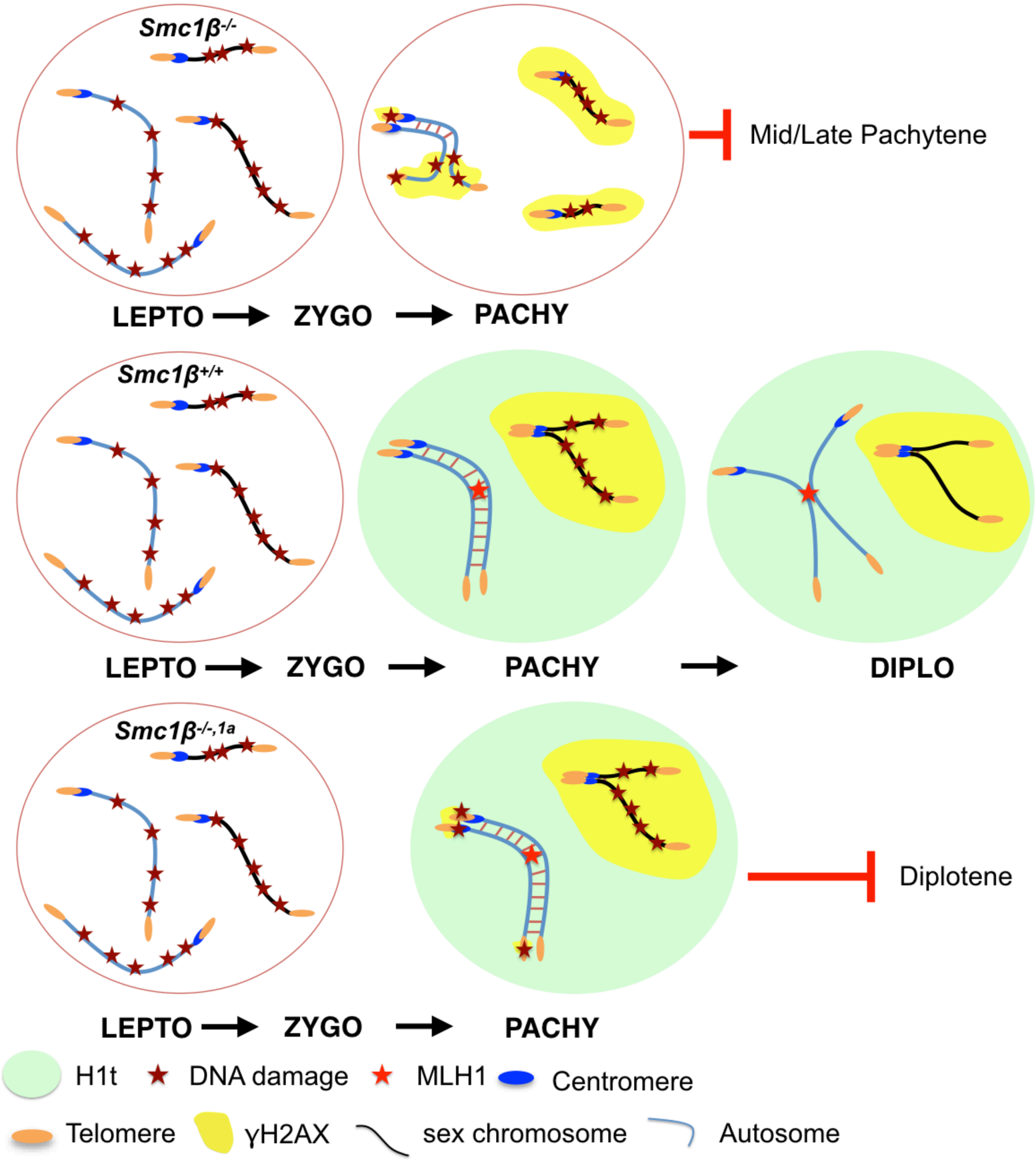
Smc1β-/-
Mid/Late Pachytene
LEPTO
ZYGO
PACHY
Smc1β+/+
LEPTO
ZYGO
PACHY
DIPLO
Smc1β-/-,1a
LEPTO
ZYGO
PACHY
Diplotene
H1t
DNA damage
MLH1
Centromere
Telomere
γH2AX
sex chromosome
Autosome

Figure S7. Telomere analysis. Related to all Figures. Summary model of the roles of SMC1α and SMC1β in spermatocytes.